2005

# Influence of a Hailstreak on Boundary Layer Evolution

Zewdu T. Segele
*Cooperative Institute for Mesoscale Meteorological Studies & School of Meteorology, Norman*

David J. Stensrub
*NOAA/National Severe Storms Laboratory, Norman*, David.Stensrud@noaa.gov

Ian C. Ratcliffe
*University of Nebraska, Lincoln*, iratcliffe2@unl.edu

Geoffrey M. Henebry
*University of Nebraska, Lincoln*, geoffrey.henebry@sdstate.edu

# Influence of a Hailstreak on Boundary Layer Evolution

ZEWDU T. SEGELE

*Cooperative Institute for Mesoscale Meteorological Studies, and School of Meteorology, Norman, Oklahoma*

DAVID J. STENSRUD

*NOAA/National Severe Storms Laboratory, Norman, Oklahoma*

IAN C. RATCLIFFE AND GEOFFREY M. HENEBRY

*University of Nebraska, Lincoln, Nebraska*

(Manuscript received 3 March 2004, in final form 20 September 2004)

ABSTRACT

Severe thunderstorms developed on 20 June 1997 and produced heavy precipitation, damaging winds, and large hail over two swaths in southeastern South Dakota. Calculations of fractional vegetation coverage (scaled from 0 to 1) based upon composite satellite data indicate that, within the hailstreak region, vegetation coverage decreased from 0.50 to near 0.25 owing to the damaging effects of hail on the growing vegetation. The northern edge of the larger hailstreak was located a few kilometers south of Chamberlain, South Dakota, a National Weather Service surface observation site. Hourly observations from Chamberlain and several nearby surface sites in South Dakota are averaged over 7 days both before and after this hail event. These observations illustrate that the late-afternoon (nighttime) temperatures are 2°C higher (2°C lower) near the hailstreak after the event than before the event. Similarly, daily average dewpoint temperatures after the event are 2.6°C lower near the hailstreak. These changes are consistent with the influences of a recently devegetated zone on changes to the surface energy budget.

To explore how these hailstreaks further affected the evolution of the planetary boundary layer in this region, two model simulations are performed using the fifth-generation Pennsylvania State University–National Center for Atmospheric Research (PSU–NCAR) Mesoscale Model (MM5). In the control run, climatology is used for the land surface characteristics, and hence the simulation is independent of the hailstreaks. In the hailstreak simulation (HSS), the fractional vegetation coverage and soil moisture in the hailstreak regions are modified to reflect the likely conditions within the hailstreaks. Two different days are simulated: one with low surface wind speeds and one with stronger surface wind speeds. For the low surface wind speed case, the HSS simulation produces a sea-breeze-like circulation in the boundary layer by midmorning. For the stronger surface wind speed case, this sea-breeze-like circulation does not develop in the HSS, but the simulated low-level temperatures are modified over a larger area. These results suggest that to capture and reasonably simulate the evolution of boundary layer structures, there is a need for routine daily updates of land surface information. Hailstreaks also are important to consider in the future as the focus for observational studies on nonclassical mesoscale circulations.

## 1. Introduction

Hail is a rare extreme weather event that can cause substantial damage to property, including crops. In the United States, the upper Great Plains and the Midwest are the principal high hail incidence areas, with hail frequencies greater than 60 hail days per 20 yr (Changnon 1984), and are where the average annual crop damage by hail is the largest in the United States (Changnon 1972, 1977; Hillaker and Waite 1985). One of the highest hail incidence regions is the Black Hills area in South Dakota, where the average frequency of hail is about 4 hail days per year based on point frequencies (Changnon 1977, 1984). The average number of days on which damaging hail occurs in South Dakota during the growing season (the 153 days from May through September) is 51, with the majority of the damaging hail days occurring in July (Frisby 1963). Both hail frequency and crop damage by hail peak in the upper Great Plains during June and July (Changnon and Stout 1967; Henebry and Ratcliffe 2003).

Hail damage to crops depends on such characteristics as number of hail falls per unit area, hail frequency, hail

*Corresponding author address:* Dr. David J. Stensrud, National Severe Storms Laboratory, 1313 Halley Circle, Norman, OK 73069.
E-mail: David.Stensrud@noaa.gov

stone size and the associated winds, crop type, and the plant's stage of growth (Sanchez et al. 1996; Changnon 1997). The extent of crop damage also depends on the spatial extent of the damaging hail event, which in turn depends on the characteristics of the hail-producing storm and the ambient environment. Crop damage generally accounts for the major portion of the total losses from hail (Hillaker and Waite 1985). Nationwide, the mean annual loss of crop and property due to hail damage is estimated at $2.3 billion, of which $1.3 billion loss results from crop damage by hail (Changnon 1997). However, hail is not the primary weather-related crop loss factor in most parts of the United States (Changnon 1972; Kunkel et al. 1999).

Hail often falls in well-organized swaths that are 8–24 km wide and 160–320 km long (Frisby 1963). These swaths tend to comprise two or more hailstreaks (areas of hail that are continuous in space with temporal coherence) that are separated by no more than 32 km during 12 h or less. These hailstreaks can have different orientations (Chagnon 1970). Frisby (1963) notes that many hail swaths across the northern Great Plains lie from northwest to southeast in the same direction as the polar front jet. Henebry and Ratcliffe (2003) identify 112 events of significant hailstreaks from 1990 to 1999 and also note that most of the hailstreaks in the upper Great Plains are oriented from northwest to southeast. They also find that hailstreak devegetated zones, as identified from satellite data, have median values for length of 66 km, area of 408 $km^2$, and persistence of 34 days. The largest hailstreak they report has an area of 8443 $km^2$, and the longest persistence of the contrast in satellite-derived Normalized Difference Vegetation Index (NDVI) values is 94 days!

In addition to the direct economic loss that crop damage from hail incurs, devegetation of the land surface by hailstreaks can have significant biogeophysical consequences. Trees and shrubs are stripped of leaves, grasses are beat down and torn, and seeds are shattered (Klimowski et al. 1998). Some of these damaged plants never recover. The hail-damaged vegetation that does recover initially produces less transpiration, owing to the reduction in the number of healthy leaves, and more bare ground is exposed directly to the sun (see Kessler and White 1981). This quickly alters the partitioning of the surface sensible and latent heat fluxes in comparison with conditions prior to the hail event, but can have longer-term implications as well.

The destruction of the vegetation that hail produces is very relevant to the atmosphere because of the many land surface–atmosphere connections (Anthes 1984). Surface characteristics such as vegetation cover, soil moisture, and surface roughness affect the energy and mass exchange between the ground surface and the lower part of the atmosphere and control the relative amounts of heat and moisture added to the atmosphere in a given location (Li and Avissar 1994; Rabin et al. 1990). Based on numerical simulation results, Crawford et al. (2001) report that soil moisture and the coverage and thickness of green vegetation have large effects on the magnitudes of surface sensible heat fluxes, while surface albedo and roughness length are of secondary importance. Substantial gradients in sensible heating resulting from contrasts in vegetation cover can modify existing mesoscale circulations or can result in the onset of thermally induced sea-breeze-like circulations, also known as land or vegetation breezes, that may trigger convection and lead to severe weather (Segal et al. 1988; Clark and Arritt 1995).

This paper examines the limited observational data to explore the effects of the 20 June 1997 hailstreaks on the surrounding environment. Once the influences of the hailstreaks are determined, two mesoscale model simulations are used to study in more detail the role of the hailstreaks on boundary layer development. Two different days are simulated, one with low surface wind speeds and one with stronger surface wind speeds. Section 2 summarizes the 20 June hailstreaks and contrasts temperature and moisture observations before and after the hail event. The basic characteristics of the mesoscale model and the model simulations are given in section 3. Section 4 presents the results of the model simulations, with a concluding discussion in section 5.

## 2. June 1997 hailstreak

According to National Climatic Data Center (NOAA 1997), several supercell thunderstorms produced large hail and damaging winds during the early-morning hours of 20 June 1997 across southeastern South Dakota. Hail up to the size of baseballs and winds gusting to 36 m $s^{-1}$ damaged and destroyed thousands of acres of crops (corn and soybeans) and downed many trees. The most extensive crop damage was to farms and ranches over southeastern South Dakota where there was a 32-km-long and a 6.4-km-wide path of near-total destruction. Hail and heavy rains were reported in central South Dakota extending to the western most edge of the hailstreak on 20 June.

These hail events left two nearby swaths of devegetated areas that can be identified on biweekly composite images of NDVI, defined as the ratio of the difference to the sum of near-infrared radiance and visible radiance (Chang and Wetzel 1991). The data are obtained from the Advanced Very High Resolution Radiometer (AVHRR) onboard the National Oceanic and Atmospheric Administration's (NOAA) polar-orbiting satellites, although the data are composited by the U.S. Geological Survey. Data from two biweekly periods can be compared to identify hailstreaks (Henebry and Ratcliffe 2003). A map of the temporal difference in NDVI from late June (Fig. 1) clearly shows two hailstreaks in South Dakota, and the overlaid hail reports indicate the ability of this approach to capture the continuity of the hail devegetated zone. The larger hail-

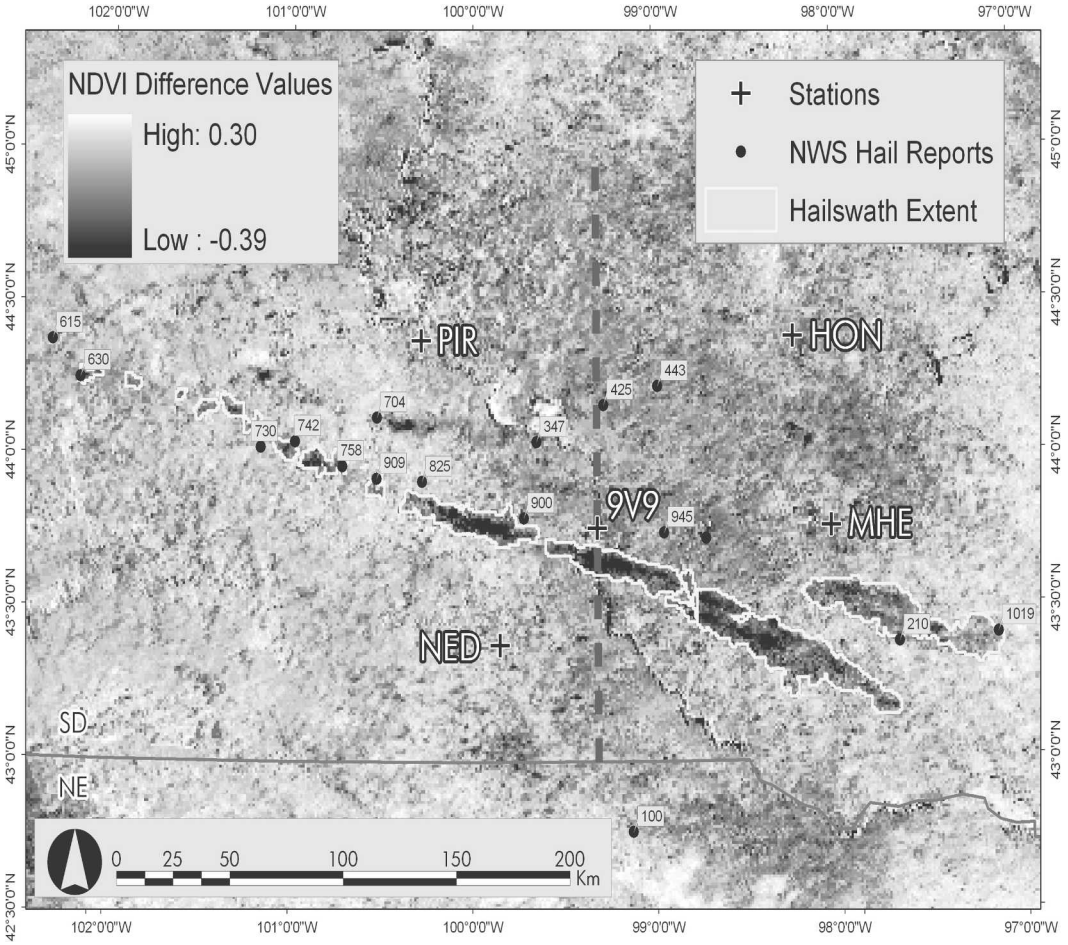


FIG. 1. Temporal difference in the NDVI between successive compositing periods bracketing the hail event over South Dakota on 20 Jun 1997. Overlaid are hail reports indicating the time of hail occurrence (UTC). and station locations as discussed in the text. Dashed line is location of cross section shown in Fig. 2.

streak covers an area more than 3° longitude (260 km) in length and, at some points, 0.20° latitude (22 km) in width. The smaller, northern hailstreak covers an area 1° longitude (87 km) in length and again up to 0.20° latitude in width.

The fractional green vegetation coverage (fVEG) can be calculated directly from the NDVI data using the method of Chang and Wetzel (1991). A north-to-south cross section of fVEG through the hailstreak along 99.32°W illustrates the effects of the hailstreak (between 43.6° and 43.7° latitude). While the vegetation coverage across the hailstreak width is uneven, owing to the varying damage to the vegetation from the hail (Fig. 2), the values of fVEG are as low as 0.25 within the hailstreak, where there was significant crop damage. This value represents up to a 50% reduction in vegetation coverage within the hail region compared to conditions prior to the hail event (Fig. 2).

One reason for exploring the effects of this hail event in more detail is that the Chamberlain, South Dakota (9V9), National Weather Service (NWS) surface observing station is located only a few kilometers north of the northern edge of the larger hailstreak. Thus, to investigate the effects of the hailstreak on the atmosphere, the near-surface temperature and moisture observations before and after the hail event at 9V9 are compared with surface observations at nearby locations that are not adjacent to the hailstreak. Hourly temperatures and dewpoint temperatures are averaged over 7-day periods from 13 to 19 June and 25 June to 1 July 1997, representing the conditions before and after the hail event, respectively. A 5-day period after the hail event is used to allow the soil to dry and the effects of the devegetated zone to become more apparent. The surface winds are typically from the south during these two 7-day periods, suggesting that the observations at 9V9 may capture some of the effects of the hailstreak.

Before the hail event, comparisons of the 7-day average hourly temperatures and dewpoint temperatures at 9V9 with those at Huron (HON), Mitchell (MHE), Winner (NED), and Pierre (PIR), South Dakota, indicate that the diurnal temperature cycles are in relatively

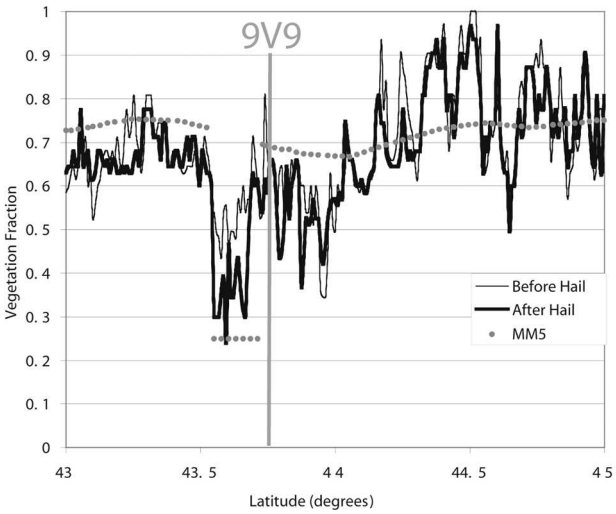


FIG. 2. South-to-north cross section of fractional green vegetation coverage as determined from composite satellite data and as represented in the model simulations across the hailstreak devegetated zone through 9V9 (at 43.8°N). Latitude of 9V9 is indicated. Location of cross section shown in Fig. 1.

close agreement (Fig. 3). While the nighttime temperatures at 9V9 are slightly cooler than those at HON and MHE (less than 1.5°C difference) and slightly warmer than those at NED and PIR (less than 1.0°C difference), the daytime temperatures are quite similar and are nearly identical for 9V9, HON, and PIR. More variability is found in the 7-day average hourly dewpoint temperatures, with similar dewpoint values at 9V9 and MHE and lower dewpoint values at 9V9 than at HON, NED, and PIR (Fig. 3). However, at 9V9, NED, and PIR the diurnal cycle of dewpoint temperature largely parallel each other, with the values at 9V9 being on average 1.9°C (1.8°C) lower than NED (PIR). Thus, there are no striking differences between the diurnal cycles of average hourly temperature and dewpoint temperature at 9V9 and its nearby stations.

In contrast, comparisons of the 7-day average hourly temperatures and dewpoint temperatures after the hail event at 9V9 and its nearby stations show diurnal cycles that are distinctly different (Fig. 4). The nighttime temperatures at 9V9 show faster cooling, and generally a lower minimum temperature at an earlier time, when compared to the other stations. In particular, at 0800 UTC the temperatures at 9V9 are at least 2°C cooler than those at MHE, HON, NED, and PIR. This situation is reversed late in the day when the temperatures near 2200 UTC are 2°C warmer at 9V9. Thus, the diurnal temperature range at 9V9 is larger than at the nearby stations after the hail event. Comparisons of the dewpoint temperatures of all the stations (Fig. 4) indicate that 9V9 is drier than the surrounding sites, and this dryness is greater than observed prior to the hail event (cf. Figs. 3 and 4). This behavior is consistent with the expectations from a nonsaturated land surface that has less actively transpiring vegetation than found in surrounding areas, since with less vegetation the surface sensible heat flux should be larger, leading to warmer daytime maximum temperatures and lower dewpoint temperatures (Segal et al. 1988; Rabin et al. 1990). In addition, a less vegetated and drier land surface should also cool faster and likely reach a cooler minimum temperature. Thus, the hourly average surface observations at 9V9 are consistent with the effects of devegetation that a hailstreak would produce at the ground surface.

Segal and Arritt (1992) conduct a simple scaling analysis to determine when a land-breeze circulation, what they call a nonclassical mesoscale circulation, would be expected. For various values of sensible heat flux and background wind speed, they calculate the estimated width of a perturbed surface zone that is needed to be able to influence the background flow. For a sensible heat flux of 200 W $m^{-2}$ and wind speeds below 3 m $s^{-1}$, the perturbed surface zone only needs to be 10 km in width for a land breeze to develop. This width increases to near 30 km for wind speeds of 5 m $s^{-1}$ and to over 50 km for wind speeds of 8 m $s^{-1}$. The perturbed surface zone width increases as the wind speed increases, because the atmosphere must respond to the induced pressure perturbations before the air is advected across the perturbed surface area. Since the devegetated area associated with the hailstreaks is roughly 15 to 20 km in width, the development of a land-breeze circulation is at least a reasonable expectation on days with wind speeds below 4 m $s^{-1}$ or so.

Unfortunately, the available surface observations are not sufficient to determine convincingly if a land breeze is present on any of the days after the 20 June hail event, since the observing stations are so widely spaced in comparison to the size of the individual hailstreaks. This lack of observational data at the scales needed to observe land breezes has been, and remains, an obstacle to improving our understanding of these features (Segal and Arritt 1992). Thus, to explore how these hailstreaks may have influenced the boundary layer in greater detail, and over a broader region, a numerical model simulation is needed.

## 3. Model description

The model used for this study is the nonhydrostatic fifth-generation Pennsylvania State University–National Center for Atmospheric Research (NCAR) Mesoscale Model (MM5, version 3.6; Dudhia 1993). The model is configured to run using 30 vertical levels (13 levels below 800 hPa) and four horizontal domains with grid sizes of 27, 9, 3, and 1 km (Fig. 5), where the domains are nested with two-way interaction. The coarse domain covers much of the United States and uses a 90-s time step. The inner domains generally are centered over south central South Dakota where the

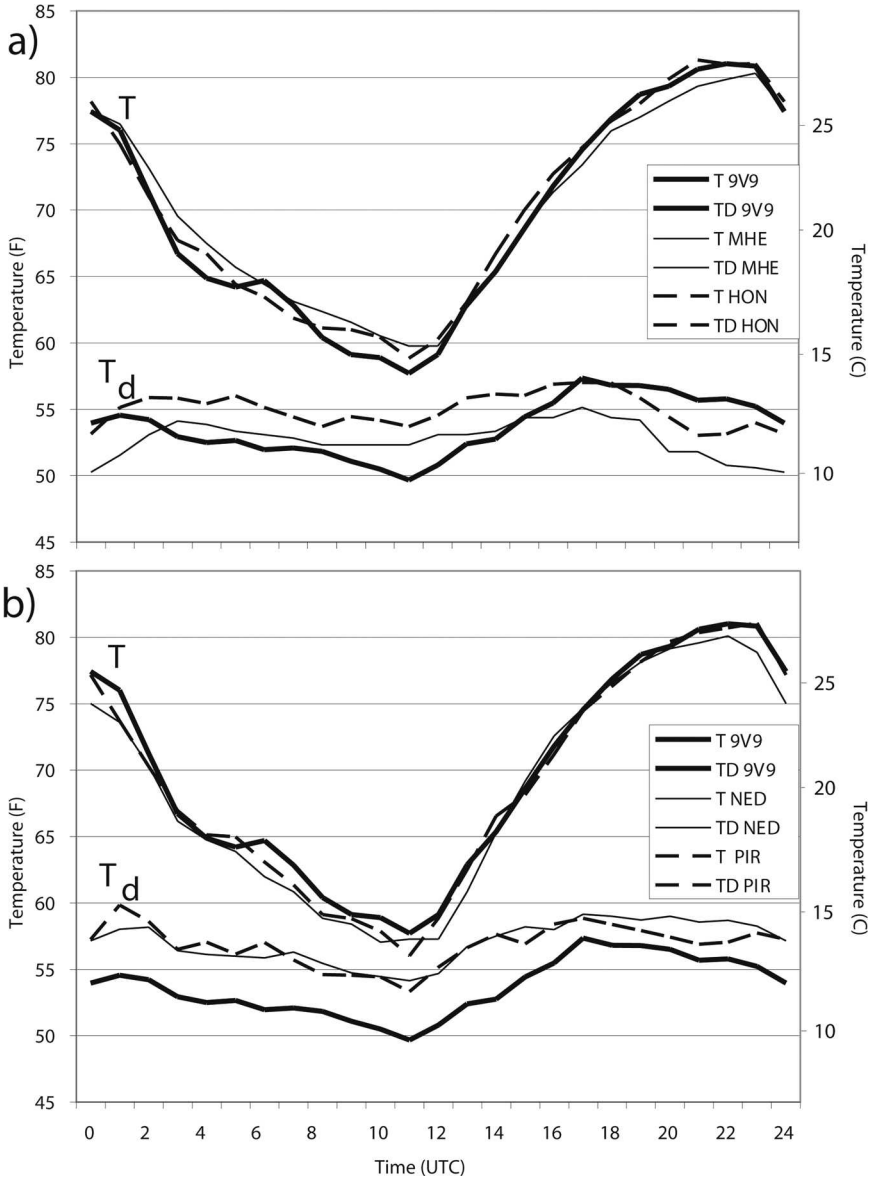


FIG. 3. Seven-day average temperatures ($T$) and dewpoint temperatures ($T_d$) from (a) 9V9, MHE, and HON and (b) 9V9, NED, and PIR prior to the 20 Jun 1997 hail event (13–19 Jun). Thick solid lines are for 9V9 in both plots, while the key indicates the other line definitions.

hailstreaks are located. Domain 3 encompasses the entire region affected by the hailstreaks, while domain 4 only encompasses part of the hailstreaks.

The model physics includes a simple ice microphysics (Dudhia 1989) and the Rapid Radiative Transfer Model (RRTM) longwave scheme (Mlawer et al. 1997) that combines a cloud-radiation shortwave scheme. In addition, the Medium-Range Forecast (MRF) model planetary boundary layer scheme (Hong and Pan 1996) and a land surface model (LSM) are used. The LSM makes use of vegetation and soil type in handling evapotranspiration and predicts soil moisture and temperature at four layers (Chen and Dudhia 2001), and it is nearly identical to the LSM used in the Eta Model. For the 27- and 9-km grids, the Kain–Fritsch (1993) convective parameterization scheme is used, but no convective parameterization is active on the two innermost grids. An explicit microphysics scheme, with equations for cloud and rainwater below the freezing level and ice and snow above the freezing level, is used on all four domains (Dudhia 1989).

The model atmospheric initial conditions are created for the 27-km grid by using the National Centers for Environmental Prediction (NCEP) global analysis as a first-guess field, and then blending in all available surface and upper-air data (Benjamin and Seaman 1985).

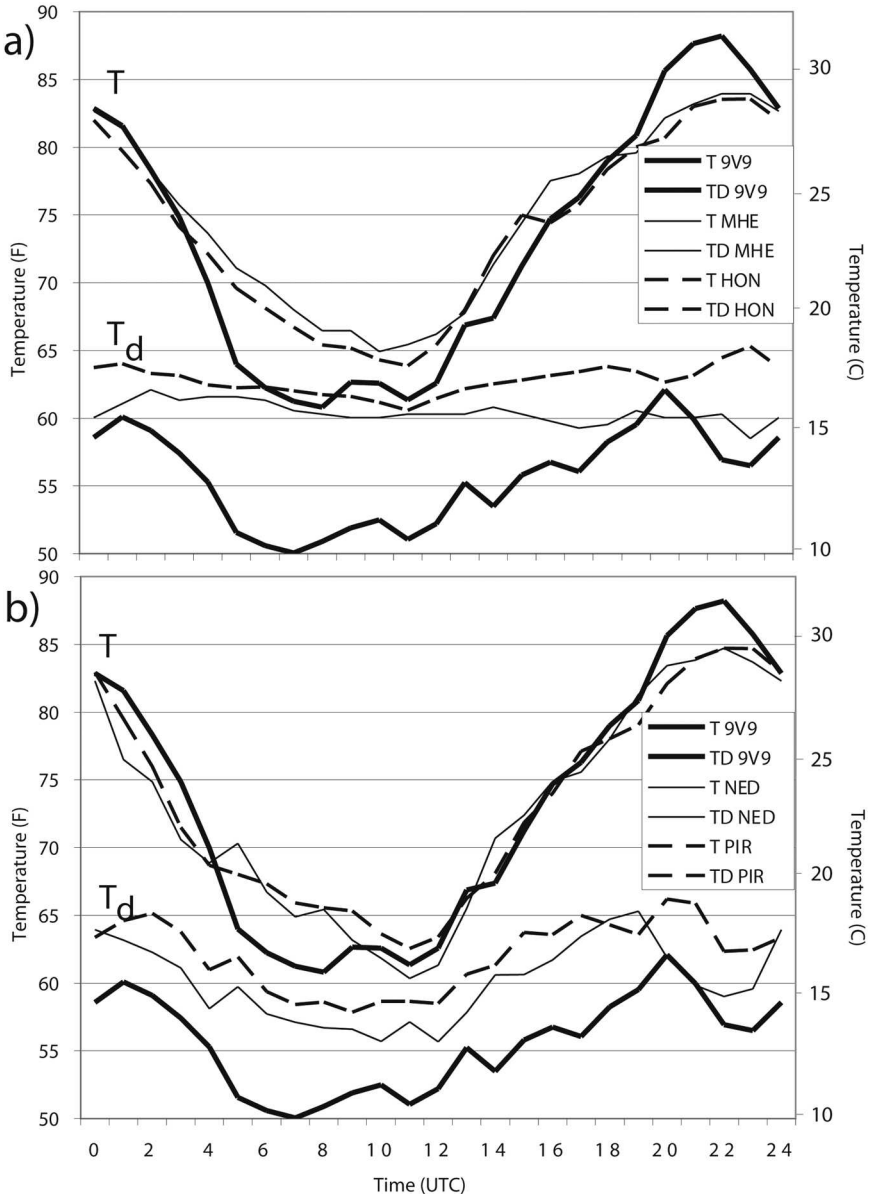


FIG. 4. As in Fig. 3, but for 7-day average values after the hail event (25 Jun–1 Jul).

Boundary conditions are provided at 12-h intervals following the same procedure. Atmospheric initial conditions for the nested grids are interpolated from the 27-km grid. The model land surface properties (albedo, emissivity, roughness length, minimum stomal resistance, hydraulic conductivity, several volumetric water content parameters, and field capacity) are specified according to 1 of 24 land-use categories for the summer season and 16 soil types, both at 1-km resolution. Thus, the land surface properties have more structure as the model grid spacing decreases. Soil moisture is estimated using an antecedent precipitation index, following Crawford et al. (2001), that uses data from over 6000 rainfall reporting stations in the United States. Values of volumetric water content estimated from this approach over the hailstreak region are generally in the range of 0.25 to 0.32 $m^3\ m^{-3}$.

To investigate the possible influences of the two hailstreaks, two different model simulations are performed on two different days. One day (28 June 1997) has low surface wind speeds over the hailstreak region (less than 4 $m\ s^{-1}$ early in the day, but increasing as the day progresses), while the other day (27 June 1997) has surface wind speeds above 6 $m\ s^{-1}$ over the hailstreak region throughout the day. All simulations start at 1200 UTC and extend out to 12 h.

Both simulation days are at least 7 days after the hail event. This is important, because Santanello and Carl-


FIG. 5. Domains used in the MM5 simulation. Domain 1 is at 27 km, domain 2 is at 9 km, domain 3 is at 3 km, and domain 4 is at 1 km resolution. Note that the devegetated zone of the hailstreak is contained completely within domain 3, but only partially in domain 4.

son (2001) indicate that rapid soil-surface drying can occur within a few days under intense sunshine, especially for lower vegetation fractions, for the uppermost 1 to 2 cm of the soil, while the deeper soil layers remain moist. This rapid drying leads to increased sensible heat flux and decreased latent heat flux from the surface. The conditions that occur after a hail event, in which vegetation fractions are small, appear to be good candidates for rapid soil drying.

The control run uses climatology for the land surface conditions, and hence it is independent of the hailstreaks. In the second simulation, we attempt to include the effects of the hailstreaks by modifying the land surface conditions within two boxes that are defined to resemble the June 1997 hailstreaks shown in Fig. 1. We realize that this is an imperfect representation of the hailstreaks, but believe it is sufficient for exploring their role in the evolution of the boundary layer on this day. In this hailstreak simulation (HSS), the climatological fractional green vegetation coverage is reduced to 0.25 and soil moisture in the uppermost soil layer for nonwater surfaces is reduced to 0.05 $m^3\ m^{-3}$ within the defined hailstreaks. While the actual values of soil moisture are unknown, this low value is chosen to approximate the likely conditions of a nearly bare ground surface after 7–8 days of late June sunshine and rapid soil-surface drying. At lower depths, the soil moisture for this simulation is again specified by the antecedent precipitation index calculations. As is shown later, these choices for fractional green vegetation and soil moisture still lead to positive latent heat flux into the atmosphere. No changes are made to other land surface parameters, such as roughness length or albedo, since these generally have a smaller influence on the resulting simulations (Crawford et al. 2001). The modifications of land surface characteristics in the HSS thus

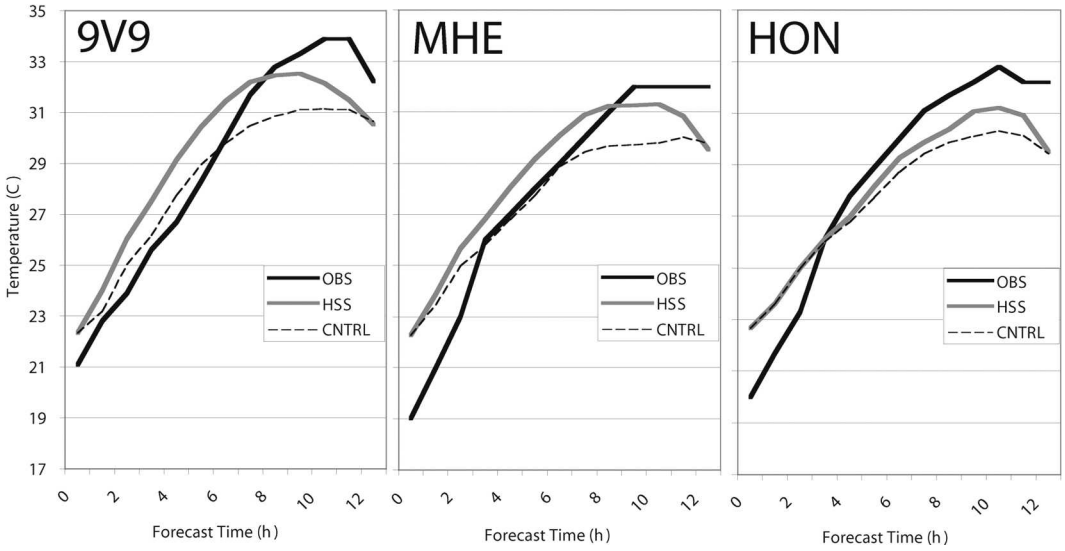


FIG. 6. Observed and model-simulated 2-m temperatures (°C) plotted vs model simulation time (h) for 9V9, MHE, and HON for the control run and HSS beginning at 1200 UTC 27 Jun 1997. Station 9V9 is closest to the hailstreak, followed by MHE and HON. Model data are from domain 3.

create a vegetation cover and soil moisture contrast that resemble the likely effects of the two hailstreaks on the ground surface.

Owing to the uncertainties in the actual soil moisture within the hailstreak regions, and the importance of the planetary boundary layer evolution to the resulting model solutions, several sensitivity tests are conducted. First, the value of soil moisture for the uppermost soil layer for nonwater surfaces is set to 0.15 $m^3$ $m^{-3}$ instead of 0.05 $m^3$ $m^{-3}$ within the hailstreak region. The soil model simulations of Santanello and Carlson (2001) suggest that 0.15 $m^3$ $m^{-3}$ is a reasonable value for soil moisture in the upper few centimeters of soil if intense sunshine only occurs for two or three days over regions with low fractional vegetation coverage. For the hailstreak cases, intense sunshine likely occurred for a few more days prior to the cases selected. Second, the value of soil moisture for the uppermost soil layer for nonwater surfaces is not altered from the control run values that take no account of the hailstreak conditions. This sensitivity test assumes that no additional drying of the soil occurred because of the reduced vegetation fraction and several days of soil drying within the hailstreak region. Third, the runs are conducted with the Eta boundary layer scheme (Janjic 1994), instead of the MRF boundary layer scheme. Results from these three sensitivity tests (not shown) are qualitatively identical to those seen with the default selections made above, although some of the simulated circulations are reduced in amplitude (particularly when the soil moisture is not altered within the hailstreak). However, the general conclusions do not change and now are discussed.

## 4. Model results

### *a. 27 June 1997*

Both model simulations (HSS and control) capture the evolution of the large-scale patterns in good agreement with the analyses at 12 h (not shown). At the surface, the model produces well the weak low over west-central South Dakota in terms of pressure pattern, trough orientation, and location. The model also correctly simulates the position of the dryline that extends northeastward from New Mexico into west Kansas, and then northward into South Dakota. At mid- to upper levels, the model-simulated geopotential height, temperature, moisture, and wind patterns are in good general agreement with the analyses. Surface winds speeds from both the model and observations in eastern South Dakota are southerly and above 5 m $s^{-1}$, so a land-breeze circulation in association with the hailstreaks is not expected according to the analysis of Segal and Arritt (1992).

One of the difficulties in evaluating the simulations is that the model provides details that are not observed, and so our assessments are based upon comparisons against a handful of observational surface data. In general, while the model and observed 2-m dewpoint temperatures and 10-m winds are in general agreement with each other when examined at selected station locations, they also have greater fluctuations from hour to hour that make comparisons more challenging. The near-surface parameter that appears to show the effects of the hailstreak most consistently at the surface is the 2-m temperature.

Both simulations underpredict the daily maximum

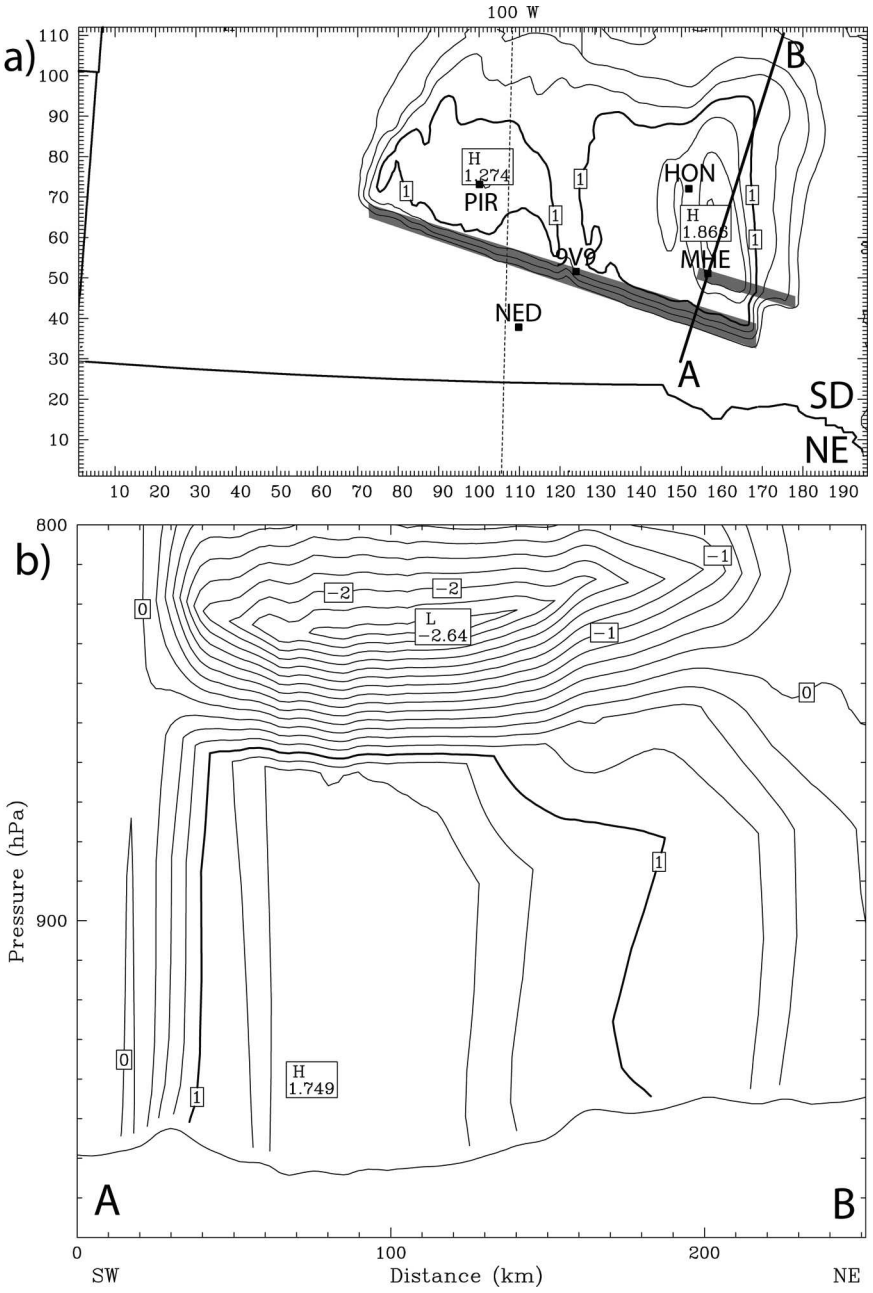


FIG. 7. Plot of (a) 900-hPa perturbation temperature (°C) at the 10-h simulation time, calculated as the HSS values minus the control run values from the 27 Jun 1997 runs. Contours every 0.25°C, starting at 0.25°C. Shaded regions indicate locations of hail devegetated zones, while thick solid line is the 1°C contour. SD and NE help indicate the South Dakota (SD) and Nebraska (NE) state boundaries. The *x* and *y* axes indicate the grid points from the model domain. (b) Cross section of perturbation temperature (°C) at the 10-h simulation time. Cross section indicated in (a) as the line AB. Contours every 0.25°C. Data are from domain 3.

2-m temperatures by at least 2°C when compared against observations at the five NWS sites in South Dakota (9V9, MHE, HON, PIR, and NED) previously discussed. In particular, the simulated early-morning temperatures are too warm, and the late-afternoon temperatures too cold, compared to observations. However, differences between the control and HSS simulations are seen at locations north of the hail-streaks (Fig. 6). The HSS simulation produces a 2-m temperature that is 1.6°C warmer than the control at 9V9, 1.4°C warmer than the control at MHE, and 0.9°C warmer than the control at HON. The effect of the

hailstreak is greatest for the station closest to the hailstreaks (9V9) and decreases with distance away from the hailstreaks. There are no differences between the HSS and control simulation temperatures at NED, located south of the hailstreaks. Thus, the addition of the hailstreaks to the model initial condition yields a simulation of 2-m temperature that is closer to the available observations in eastern South Dakota. In addition, the increase in 2-m temperature at 9V9 from the HSS as compared with values from the control run is roughly of the same magnitude as the increase in observed temperature at 9V9 compared to the surrounding surface stations when averaged over 7 days in the period after the hail event. This suggests that the magnitude of the simulated increase in temperature near the hailstreak seen in the HSS appears to be reasonable.

As expected, the model simulation shows no indication of a land-breeze circulation (not shown). However, the temperature differences between the HSS and control simulations extend across a relatively large area (Fig. 7a). The HSS simulation is warmer at 900 hPa by up to 1.8°C, while the values of mixing ratio in the HSS are lower than the control by up to 3 g $kg^{-1}$ at this same level (not shown). Note that the changes in 900-hPa temperature are largest downstream of the two hailstreaks in comparison with the differences farther west where only one hailstreak is present. A cross section through this region shows that the HSS is warmer than the control run below 850 hPa, and cooler above 850 hPa (Fig. 7b), owing to the deeper boundary layers produced in the HSS. The effect on the mixing ratio is reversed, with the HSS generally being drier below 850 hPa and moister above when compared against the control (not shown).

### *b. 28 June 1997*

Both model simulations (HSS and control) again produce a reasonable reproduction of the evolution of the synoptic-scale features during the 12-h period of simulation starting at 1200 UTC 28 June 1997. The surface wind speeds on this day are weaker than those on 27 June, since the weak surface low pressure system is located over west-central South Dakota and the pressure gradient in the central and eastern portions of the state is more relaxed. Both model and observed surface winds are generally light and southwesterly (less than 4 m $s^{-1}$ during most of the day), so the analysis of Segal and Arritt (1992) suggests that a land-breeze circulation may be produced.

Again, comparisons are focused upon the simulated and observed 2-m temperatures at the five sites closest to the hailstreak region. The model underpredicts maximum 2-m temperatures typically by between 2° and 3°C, with the predicted temperatures very nearly the same in both the HSS and control simulations except at 9V9 and MHE. For these two sites, the HSS simulation is warmer, and compares better with the observations (Figs. 8a,c), than the control. Since these two stations are located downwind from the hailstreaks, and are the closest stations to the hailstreak region, it appears that the devegetated zones within the hailstreaks lead to warmer temperatures through increased sensible heat flux in these zones where the vegetation is damaged and has a smaller fractional coverage. Again,

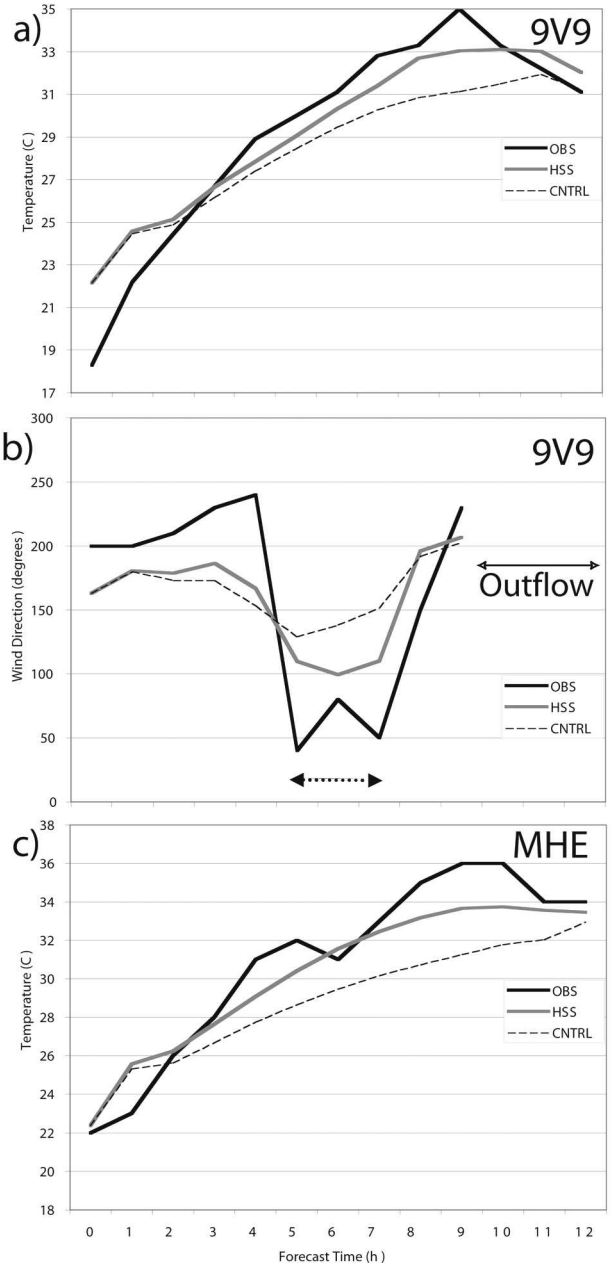


FIG. 8. Observed and model-simulated 2-m temperature for (a) 9V9 and (c) MHE vs simulation time (h) for the control run and HSS beginning 1200 UTC 28 Jun 1997. (b) Observed and model-simulated wind direction at 9V9 vs simulation time (h). Note the dramatic change in observed wind direction between hours 5 and 7. Also note that a weak outflow from convection to the north is suggested in the data beginning at 10 h, and so no winds are plotted after this time. Model data are from domain 3.

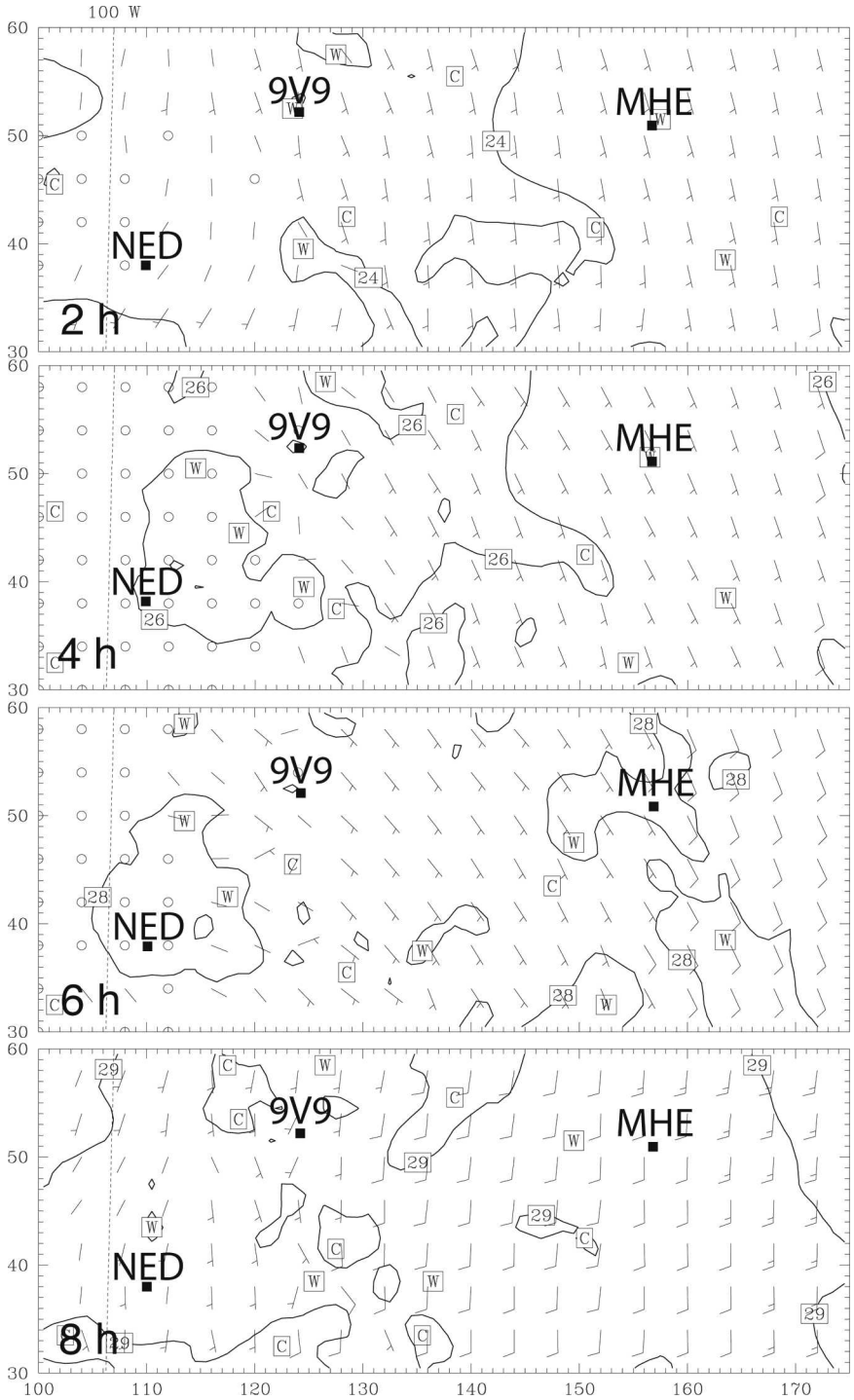


FIG. 9. Plots of lowest sigma layer temperature (°C) and winds from control run started at 1200 UTC 28 Jun 1997 from 2-, 4-, 6-, and 8-h simulation times. Contours of temperature every 1°C. Locations of Chamberlain (9V9), Mitchell (MHE), and Winner (NED) are shown. Full wind barb is 5 m $s^{-1}$. Output is from model domain 3.

the simulated 2-m temperature increases at 9V9 seen in the HSS are comparable to those observed at 9V9 in comparison to the other observing stations when averaged over a 7-day period after the hail event. This suggests that the magnitude of the 2-m temperature increase seen in the HSS again is reasonable.

The wind direction at 9V9, the station closest to a hailstreak, also is suggestive of the effects of the deveg-

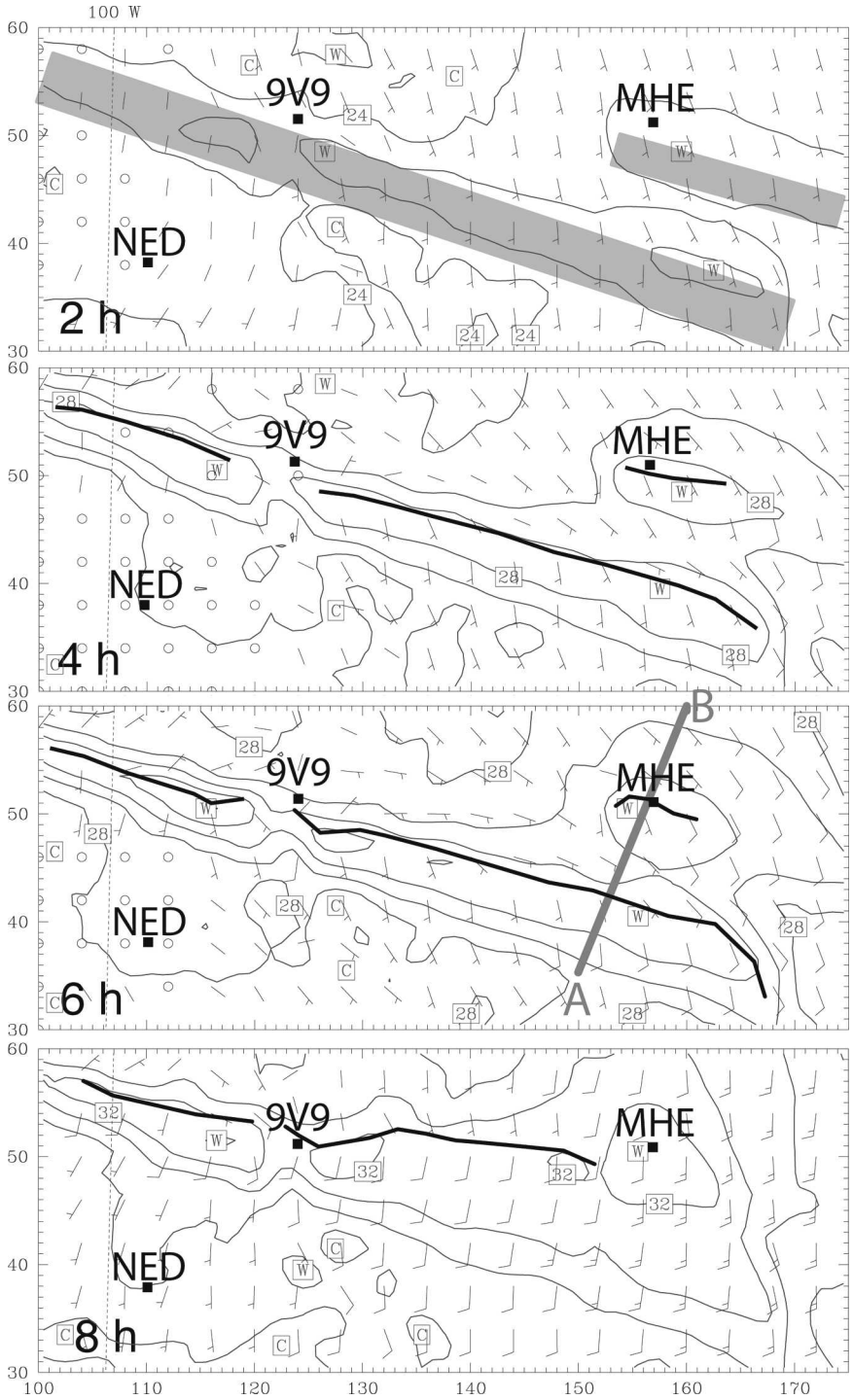


FIG. 10. As in Fig. 9, but for the HSS. Shaded regions in 2-h plot denote hailstreak devegetated zones. Thick black lines in 4-, 6-, and 8-h plots indicate location of the land-breeze front. Thick gray line with labels "A" and "B" in 6-h plot indicates location of cross section shown in Fig. 12.

etated zones on this day with weaker surface wind speeds. Both observations and model simulations indicate a more easterly component to the winds between 5 and 7 h (1700 to 1900 UTC) that is more prevalent in the HSS than in the control (Fig. 8b). Wind speeds are less than 2 m $s^{-1}$ during this time period. Since the hailstreak devegetated zone is located to the south of 9V9, this easterly wind (northeasterly in the observa-

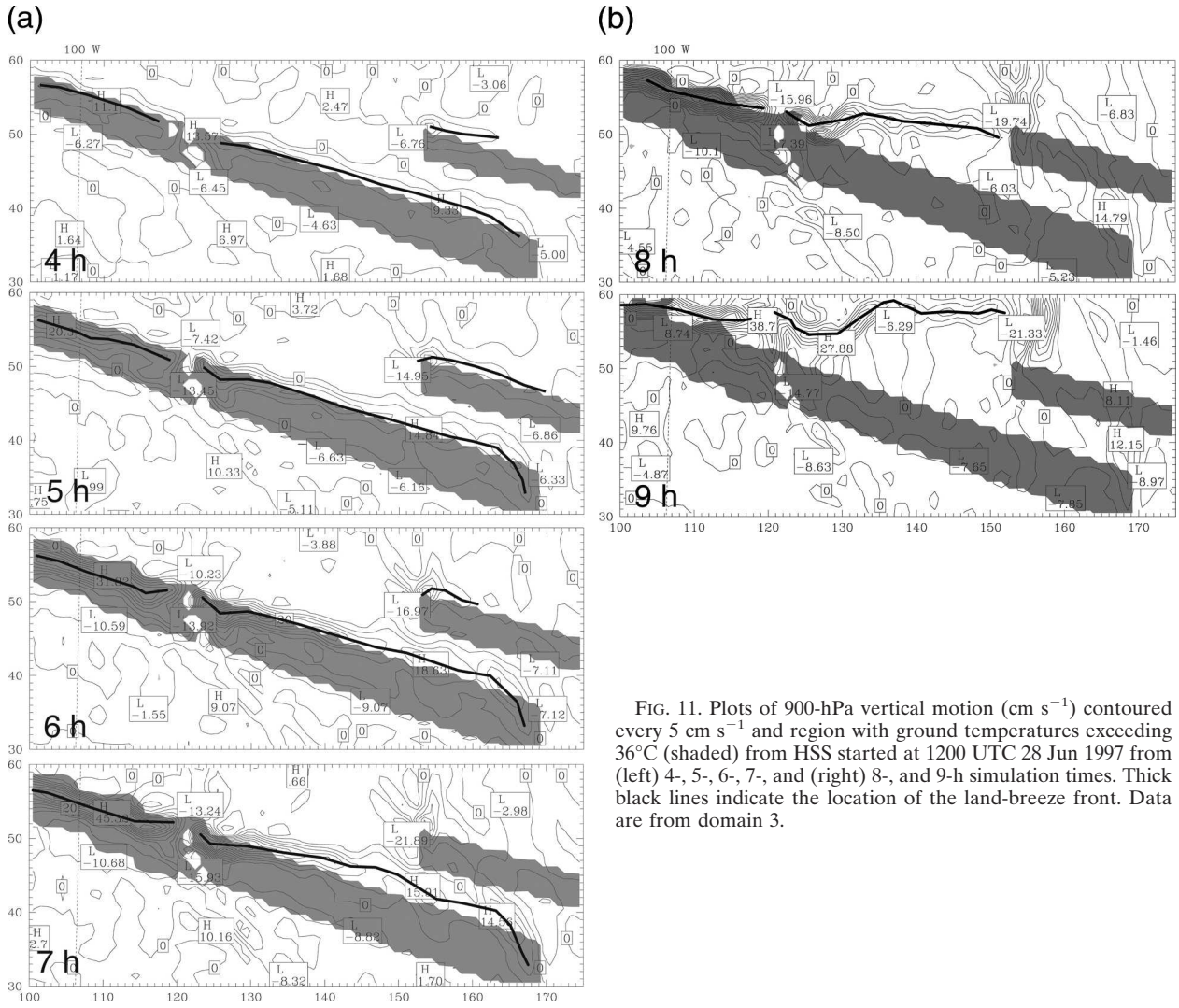


FIG. 11. Plots of 900-hPa vertical motion (cm $s^{-1}$) contoured every 5 cm $s^{-1}$ and region with ground temperatures exceeding 36°C (shaded) from HSS started at 1200 UTC 28 Jun 1997 from (left) 4-, 5-, 6-, 7-, and (right) 8-, and 9-h simulation times. Thick black lines indicate the location of the land-breeze front. Data are from domain 3.

tions) may be a response to the lower surface pressure that develops over the hailstreaks owing to the increased sensible heat flux and warmer boundary layer temperatures. This easterly wind even may be an indication that a land-breeze circulation is present at this time. A closer examination of the model output is needed to ascertain what is producing these more easterly winds in the HSS.

The control simulation produces southerly to southeasterly surface winds across the hailstreak region throughout the day (Fig. 9). Wind speeds remain generally light until late in the day (8 h) when speeds increase to slightly above 5 m $s^{-1}$. In contrast, surface winds from the HSS are much more easterly across the central portion of the domain (Fig. 10), to the north of the hailstreaks, starting at 4 h. There even is a northeasterly wind at a location just to the east of 9V9 at 4 and 6 h. Clearly, the HSS is capturing a feature that is not seen in the control simulation and that reproduces more accurately the fairly dramatic changes in the observed wind direction at 9V9. This feature is a land-breeze circulation. While the observational data alone are not sufficient to verify that a land-breeze circulation existed on this day, the development of easterly winds is unusual and so we explore the model data to see why these winds occurred in the simulation.

Initially, ground temperatures across the hailstreak region are slowly varying in space owing to the relatively smooth initial condition. However, within a few hours the temperatures within the hailstreak region are several degrees Celsius warmer than the surrounding areas. By 4 h, a land-breeze circulation is seen clearly in the model output (Fig. 11). The zone of rising motion at 900 hPa is already located along the northern edge of the hail-produced devegetated zones, owing to the effects of the background southerly low-level winds. This zone of rising motion defines the edge of the region affected by the land breeze and is called the land-breeze front. As the simulation progresses, the zone of rising motion intensifies until it reaches a maximum

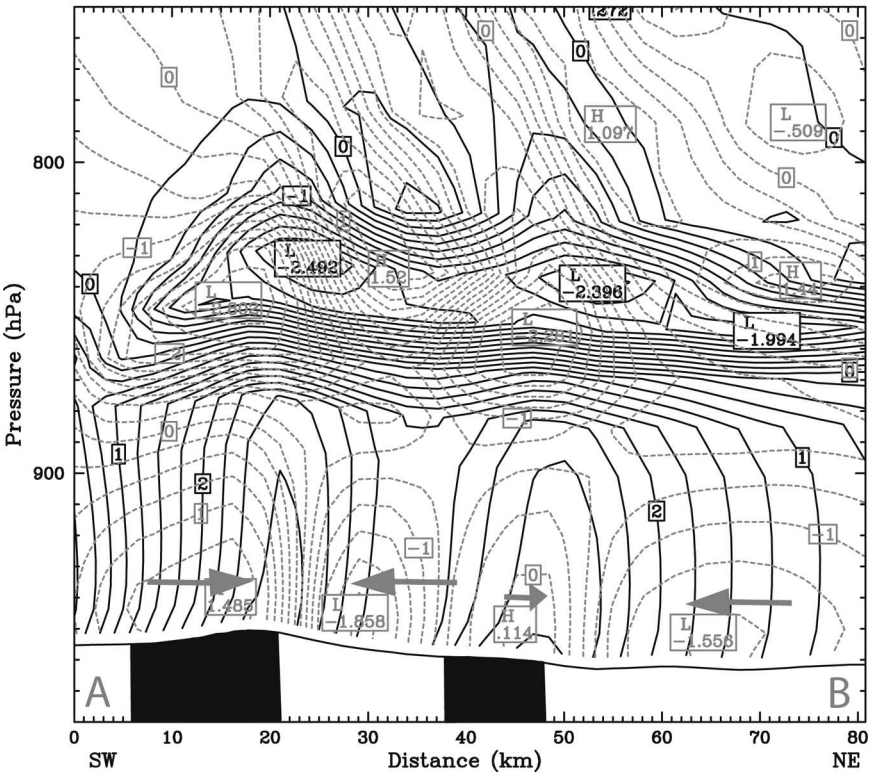


FIG. 12. Cross-section plots of perturbation temperature (°C; solid lines) and perturbation wind speed (m $s^{-1}$; dashed lines) parallel to the cross section as functions of pressure (hPa), calculated as HSS values minus control run values at the 6-h simulation time from the 28 Jun 1997 runs. Contours of perturbation temperature every 0.25°C and wind speed every 0.25 m $s^{-1}$. Location of the cross section is shown in Fig. 10. Arrows denote low-level perturbation wind flow. Black zones below terrain indicate hailstreak locations. Data are from domain 3.

near 7 h of over 45 cm $s^{-1}$ on domain 3 ($w$ approaches 1 m $s^{-1}$ on domain 4). With the weak environmental winds, the land-breeze front remains close to the hailstreaks.

A cross section through the land breeze at 6 h shows that temperatures throughout the lower boundary layer in the HSS are 1°C warmer than the control run over a 70-km-wide zone and are over 2°C warmer over two 15-km-wide regions (Fig. 12). Above this warm low-level perturbation the atmosphere in the HSS is cooler than in the control run owing to the deeper boundary layers that have developed (Fig. 13). Boundary layers influenced by the devegetated zone are typically 50 hPa deeper than those outside this zone. The temperature differences over the hailstreaks lead to maximum surface pressure decreases of 0.8 hPa in the HSS as compared to the control run. Segal et al. (1989) estimated surface pressure differences of 0.2 to 1.0 hPa in association with sea breezes. Differences in the component of the wind parallel to the cross section show the response of the wind field to these pressure perturbations. Boundary layer winds converge into the zones of warm temperature perturbations, with speeds exceeding 1.5 m $s^{-1}$ in some locations (Fig. 12). Although the patterns are slightly more complex, owing to the two zones of devegetated land surface, these circulations closely resemble those seen in other studies of land breezes that occur owing to strong gradients in soil moisture or vegetation (Ookouchi et al. 1984; Mahfouf et al. 1987; Yan and Anthes 1988; Segal et al. 1988; Schadler 1990). Thus, it appears that the devegetation effects of hailstreaks likely are sufficient to produce land-breeze circulations on some days.

An examination of the surface fluxes from a grid point within the hailstreak shows that the control run produces latent heat fluxes that peak at over 500 W $m^{-2}$, whereas the sensible heat fluxes remain at less than 150 W $m^{-2}$ (Fig. 14). This situation is nearly reversed in the HSS, where latent heat fluxes are now near 200 W $m^{-2}$ and sensible heat fluxes exceed 400 W $m^{-2}$.

The hailstreaks not only create land-breeze circulations in the model, but these circulations further alter the convective inhibition (Fig. 15a). While no convection develops in the model near the hailstreaks on this day, in agreement with observations, the convective inhibition is reduced to below 50 J $kg^{-1}$ along the zone of rising motion. In comparison to the control run, the

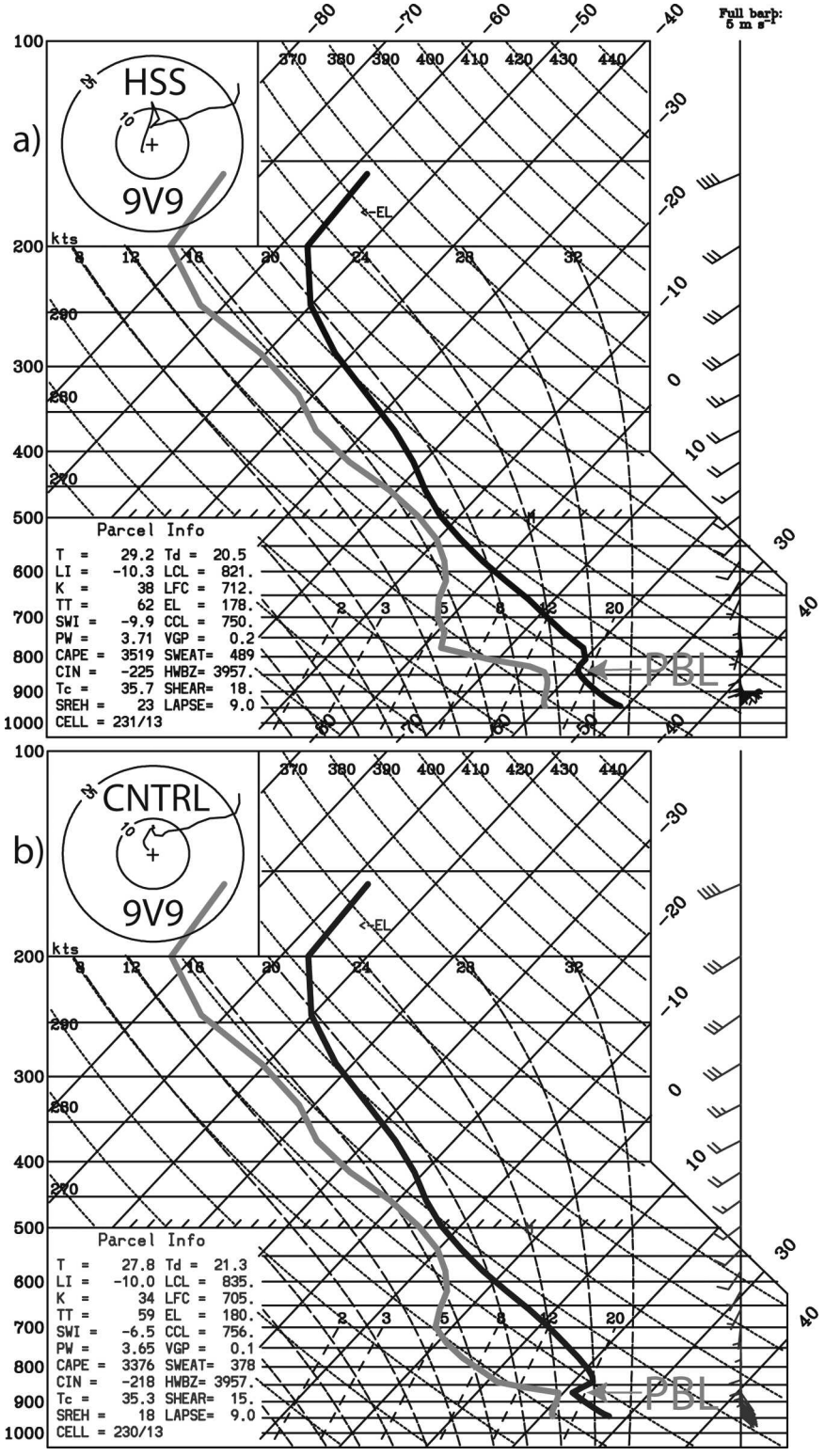


FIG. 13. Skew $T$–log $p$ diagrams from 9V9 at the 6-h simulation time in (a) the HSS and (b) the control run from the 28 Jun 1997 runs. The depth of the planetary boundary layer (PBL) is indicated by the arrow. Full wind barbs are 5 m s$^{-1}$. Data are from domain 3.

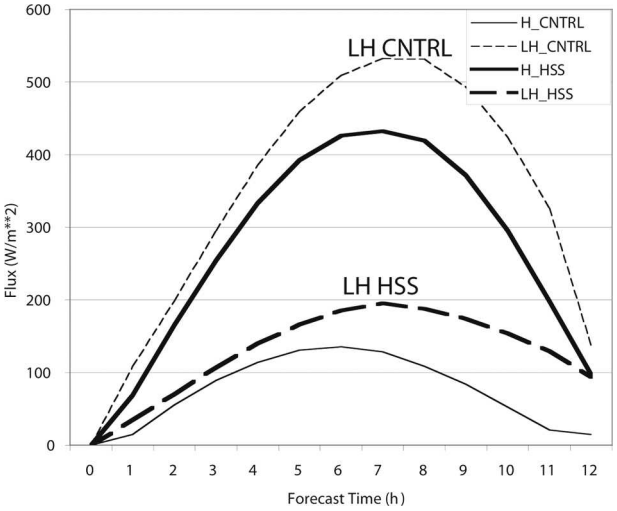


FIG. 14. Plots of latent heat (LH; dashed lines) and sensible heat (H; solid lines) fluxes (W $m^{-2}$) vs simulation time (h) from both the HSS (thick lines) and control run (thin lines) from a location within the larger hailstreak (43.63°N, 99.00°W). Data from the 28 Jun 1997 runs on domain 3.

HSS reduces convective inhibition by 20 to 30 J $kg^{-1}$ along the land-breeze front and increases convective inhibition in the regions of subsidence farther to the south (Fig. 15b). Crook (1996) indicates that differences in boundary layer temperature and moisture of 1°C and 1 g $kg^{-1}$ can lead to either the development of convection or no convection at all in cloud model simulations. The HSS shows that the devegetated zones produced by the hailstreaks are capable of creating changes in boundary layer temperature and moisture that exceed the values shown by Crook (1996) to be important. In fact, differences in 900-hPa temperature between the HSS and control runs show that the effect of the hailstreaks extend across a region significantly larger than the hailstreaks themselves, with temperature differences exceeding 1°C over an area many times the area of the hailstreaks (Figs. 7 and 16). While the hailstreaks act to warm and deepen the boundary layer, they also act to dry the boundary layer. Thus, the combined effects of the hailstreak zones on the potential for convective development is difficult to predict and likely varies from day to day.

## 5. Summary and discussion

Severe thunderstorms developed on 20 June 1997 and produced heavy precipitation, damaging winds, and large hail over two swaths in southeastern South Dakota. Calculations of fractional vegetation coverage from NOAA polar-orbiting satellite composite data in-

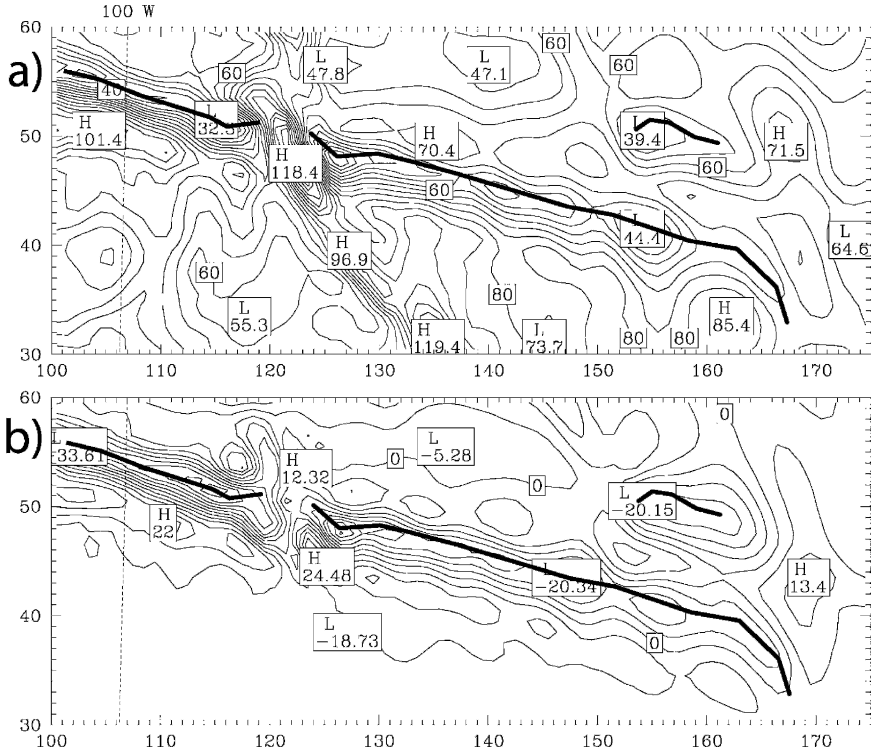


FIG. 15. Contours of (a) convective inhibition (J $kg^{-1}$) from the HSS at 6 h, and (b) perturbation convective inhibition (J $kg^{-1}$), calculated as the HSS values minus the control run values at 6 h for the 28 Jun 1997 runs. Contours in both plots are every 5 J $kg^{-1}$. Thick solid lines denote the location of the land-breeze front. Data are from domain 3.

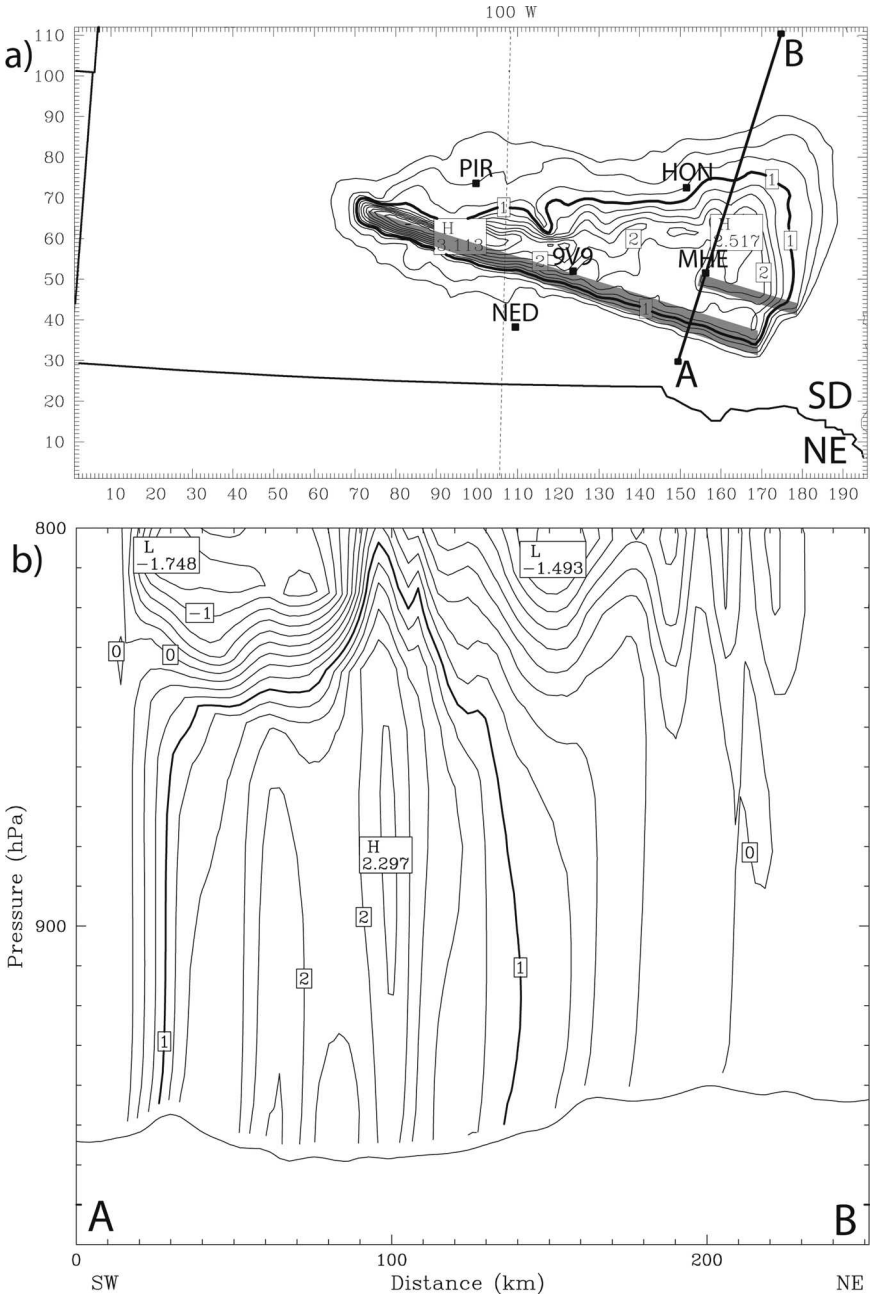


FIG. 16. Plot of (a) 900-hPa perturbation temperature (°C) at the 10-h simulation time, calculated as the HSS values minus the control run values for the 28 Jun 1997 runs. Contours every 0.25°C, starting at 0.25°C. Shaded regions indicate locations of hail devegetated zones, while thick solid line is the 1°C contour. SD and NE help indicate the state boundaries. (b) Cross section of perturbation temperature (°C) at the 10-h simulation time. Cross section indicated in (a). Contours every 0.25°C. Data are from domain 3.

dicate that vegetation coverage decreased from over 0.5 to near 0.25 in the hailstreak region owing to the damaging effects of hail on the growing vegetation. Henebry and Ratcliffe (2003) indicate that hailstreaks are most readily identifiable in croplands during summer when vegetation cover is maximal. The northern edge of the larger and more southern hailstreak was located a few kilometers south of the Chamberlain, South Dakota, NWS surface observation site. This fortuitous coincidence allows us to compare observations both before and after the hail occurrence to determine if the devegetated zone associated with the hailstreaks pro-

duced any noticeable changes in near-surface temperature and moisture.

Hourly observations from Chamberlain and several nearby surface sites in South Dakota, averaged over 7 days both before and after this hail event, indicate that the late-afternoon (nighttime) temperatures are 2°C higher (2°C lower) at Chamberlain after the event than before the event. Similarly, daily average dewpoint temperatures after the event are 2.6°C lower at Chamberlain. These changes in temperature and dewpoint temperature are consistent with the influences of a recently devegetated zone on the surface energy budget.

To explore how hailstreaks further affect the evolution of the planetary boundary layer in this region, two model simulations are performed using MM5 (version 3.6). In the control run, climatology is used for the land surface characteristics, whereas in the HSS the fractional vegetation coverage and soil moisture in the hailstreak region are modified to reflect likely conditions within the hailstreak region. These two model simulations are performed on two different days: one with weak surface winds, and the other with stronger surface winds. For the case with weak surface winds, the HSS simulation produces a land-breeze circulation in the boundary layer. This circulation develops within 3 h and remains close to the hailstreak. For the case with stronger surface winds, no land-breeze circulation is seen, although the boundary layer temperatures and mixing ratios are modified up to 70 km downwind of the hailstreaks within the 12-h period of simulation. Sensitivity tests with different values of soil moisture within the hailstreak region, and a different planetary boundary layer parameterization scheme, yield qualitatively identical results.

While the available observations are not sufficient to know with certainty that a land breeze actually occurred on the day with weak surface winds, confidence in the model simulations is gained by knowing that the model results agree with a simple scaling analysis for when a land-breeze circulation should occur. On the day with stronger surface winds, the scaling analysis suggests that a land breeze should not occur and the model is unable to produce one. On the day with weaker surface wind speeds, the scaling analysis suggests that a land breeze may occur and the model produces one. Thus, the model behavior is consistent with expectations from simple theory.

The presence of the hailstreak in the HSS did not influence the evolution of the large-scale weather pattern, but it did modify the local conditions through changes in the low-level wind field, low-level temperature and moisture values, boundary layer depth, and convective inhibition. These changes are large enough to influence the development of convection as discussed by Crook (1996). This strongly argues for routine updates of real-time land surface information so that we can capture and reasonably simulate the evolution of boundary layer features. Without routine updates, features such as devegetated zones produced by hailstreaks will go largely unnoticed. In addition, Kurkowski et al. (2003) have shown the improvements in 2-m temperature and dewpoint temperature predictions that result from routine updates to fractional vegetation coverage in the Eta Model.

Results from this study also can be interpreted to suggest that hailstreaks are a reasonable focus for observational studies of nonclassical mesoscale circulations. As mentioned in Segal and Arritt (1992), the lack of observational data on small scales has hampered our understanding of these features. Henebry and Ratcliffe (2003) indicate that devegetated hailstreak zones that are sufficiently large to be resolved with 1-km$^2$ pixels are a fairly regular occurrence in the northern Great Plains during the summer, producing alterations to the land surface that can persist for several weeks. With the mobile observing systems now available, hailstreaks seem a natural laboratory for the study of nonclassical mesoscale circulations.

*Acknowledgments.* This research was supported in part by NSF Grant EIA-0131937 to GMH. This study is also a contribution of the University of Nebraska Agricultural Research Division, Lincoln, Nebraska, Journal Series 14511. We thank three anonymous reviewers who provided constructive and helpful comments that improved this manuscript. We also thank the Information Technology Services group at NSSL for their assistance.

## REFERENCES

Anthes, R. A., 1984: Enhancement of convective precipitation by mesoscale variations in vegetative covering in semiarid regions. *J. Climate Appl. Meteor.,* **23,** 541–554.

Benjamin, S. O., and N. L. Seaman, 1985: A simple scheme for objective analysis in curved flow. *Mon. Wea. Rev.,* **113,** 1184–1198.

Chang, J.-T., and P. J. Wetzel, 1991: Effects of spatial variations of soil moisture and vegetation on the evolution of a prestorm environment: A numerical case study. *Mon. Wea. Rev.,* **119,** 1368–1390.

Changnon, S. A., 1970: Hailstreaks. *J. Atmos. Sci.,* **27,** 109–125.

——, 1972: Examples of economic losses from hail in the United States. *J. Appl. Meteor.,* **11,** 1128–1137.

——, 1977: The scales of hail. *J. Appl. Meteor.,* **16,** 626–648.

——, 1984: Temporal and spatial variations in hail in the upper Great Plains and Midwest. *J. Climate Appl. Meteor.,* **23,** 1531–1541.

——, cited 1997: Trends in hail in the United States. Proc. Workshop on Social and Economic Impacts of Weather, Boulder, CO, USWRP. [Available online at http://sciencepolicy.colorado.edu/socasp/weather1/changnon.html.]

——, and G. E. Stout, 1967: Crop-hail intensities in central and northwest United States. *J. Appl. Meteor.,* **6,** 542–548.

Chen, F., and J. Dudhia, 2001: Coupling an advanced land surface–hydrology model with the Penn State–NCAR MM5 modeling system. Part II: Preliminary model validation. *Mon. Wea. Rev.,* **129,** 587–604.

Clark, C. A., and R. W. Arritt, 1995: Numerical simulations of the effect of soil moisture and vegetation cover on the development of deep convection. *J. Appl. Meteor.,* **34,** 2029–2045.

Crawford, T. M., D. J. Stensrud, F. Mora, J. W. Merchant, and P. J. Wetzel, 2001: Value of incorporating satellite-dervied land cover data in MM5/PLACE for simulating surface temperatures. *J. Hydrometeor.,* **2,** 453–468.

Crook, N. A., 1996: Sensitivity of moist convection forced by boundary layer processes to low-level thermodynamic fields. *Mon. Wea. Rev.,* **124,** 1767–1785.

Dudhia, J., 1989: Numerical study of convection observed during the winter monsoon experiment using a mesoscale two-dimensional model. *J. Atmos. Sci.,* **46,** 3077–3107.

——, 1993: A nonhydrostatic version of the Penn State–NCAR Mesoscale Model: Validation tests and simulation of an Atlantic cyclone and cold front. *Mon. Wea. Rev.,* **121,** 1493–1513.

Frisby, E. M., 1963: Hailstorms of the upper Great Plains of the United States. *J. Appl. Meteor.,* **2,** 759–766.

Henebry, G. M., and I. C. Ratcliffe, 2003: Occurrence and persistence of hailstreaks in the vegetated land surface. Preprints, *17th Conf. on Hydrology,* Long Beach, CA, Amer. Meteor. Soc., CD-ROM, JP5.3.

Hillaker, H. J., and P. J. Waite, 1985: Crop-hail damage in Midwest corn belt. *J. Climate Appl. Meteor.,* **24,** 3–15.

Hong, S.-Y., and H.-L. Pan, 1996: Nonlocal boundary layer vertical diffusion in a medium-range forecast model. *Mon. Wea. Rev.,* **124,** 2322–2339.

Janjic, Z. I., 1994: The step-mountain Eta coordinate model: Further developments of the convection, viscous sublayer, and turbulence closure schemes. *Mon. Wea. Rev.,* **122,** 927–945.

Kain, J. S., and J. M. Fritsch, 1993: Convective parameterization for mesoscale models: The Kain–Fritsch scheme. *The Representation of Cumulus Convection in Numerical Models, Meteor. Monogr.,* No. 46, Amer. Meteor. Soc., 165–170.

Kessler, E., and G. F. White, 1981: Thunderstorms in a social context. *The Thunderstorms in Human Affairs*, E. Kessler, Ed., University of Oklahoma Press, 3–18.

Klimowski, B. A., M. R. Hjelmfelt, M. J. Bonkers, D. Sedlacek, and L. R. Johnson, 1998: Hailstorm damage observed from the *GOES-8* satellite: The 5–6 July 1996 Butte–Meade storm. *Mon. Wea. Rev.,* **126,** 831–834.

Kunkel, K. E., R. A. Pielke, and S. A. Changnon, 1999: Temporal fluctuations in weather and climate extremes that cause economic and human health impacts: A review. *Bull. Amer. Meteor. Soc.,* **80,** 1077–1098.

Kurkowski, N. P., D. J. Stensrud, and M. E. Baldwin, 2003: Assessment of implementing satellite-derived land cover data in the Eta Model. *Wea. Forecasting,* **18,** 404–416.

Li, B., and R. Avissar, 1994: The impact of spatial variability of land-surface characteristics on land-surface heat fluxes. *J. Climate,* **7,** 527–537.

Mahfouf, J. F., E. Richard, and P. Mascart, 1987: The influence of soil and vegetation on the development of mesoscale circulations. *J. Climate Appl. Meteor.,* **26,** 1483–1495.

Mlawer, E. J., S. J. Taubman, P. D. Iacono, and S. A. Clough, 1997: Radiative transfer for inhomogeneous atmosphere: RRTM, a validated correlated-k model for the longwave. *J. Geophys. Res.,* **102** (D14), 16 663–16 682.

NOAA, 1997: *Storm Data*. Vol. 39, No. 7, 347 pp. [Available online at http://www5.ncdc.noaa.gov/pdfs/sd/sd.html.]

Ookouchi, Y., M. Segal, R. C. Kessler, and R. A. Pielke, 1984: Evaluation of soil moisture effects on the generation and modification of mesoscale circulations. *Mon. Wea. Rev.,* **112,** 2281–2292.

Rabin, R. M., S. Stadler, P. J. Wetzel, D. J. Stensrud, and M. Gregory, 1990: Observed effects of landscape variability on convective clouds. *Bull. Amer. Meteor. Soc.,* **71,** 272–280.

Sanchez, J. L., R. Fraile, J. L. De La Madrid, M. T. De La Fuente, P. Rodrfguez, and A. Castro, 1996: Crop damage: The hail size factor. *J. Appl. Meteor.,* **35,** 1535–1541.

Santanello, J. A., Jr., and T. N. Carlson, 2001: Mesoscale simulation of rapid soil drying and its implications for predicting daytime temperature. *J. Hydrometeor.,* **2,** 71–88.

Schadler, G., 1990: Triggering of atmospheric circulations by moisture inhomogeneities of the earth's surface. *Bound.-Layer Meteor.,* **51,** 1–30.

Segal, M., and R. W. Arritt, 1992: Nonclassical mesoscale circulations caused by surface sensible heat flux gradients. *Bull. Amer. Meteor. Soc.,* **73,** 1593–1604.

——, R. Avissar, M. C. McCumber, and R. A. Pielke, 1988: Evaluation of vegetation effects on the generation and modification of mesoscale circulations. *J. Atmos. Sci.,* **45,** 2268–2292.

——, W. E. Schreiber, G. Kallos, J. R. Garratt, A. Rodi, J. Weaver, and R. A. Pielke, 1989: The impact of crop areas in northeast Colorado on mid-summer mesoscale thermal circulations. *Mon. Wea. Rev.,* **117,** 809–825.

Yan, H., and R. A. Anthes, 1988: The effects of variations in surface moisture on mesoscale circulations. *Mon. Wea. Rev.,* **116,** 192–208.